






ORIGINAL ARTICLE

Distinct structural and dynamic components of portal hypertension in different animal models and human liver disease etiologies

Philipp Königshofer^{1,2,3,4,5}  | Benedikt Silvester Hofer^{1,2,3,4} |
 Ksenia Brusilovskaya^{1,2,3,4,5} | Benedikt Simbrunner^{1,2,3,4,5,6}  |
 Oleksandr Petrenko^{1,2,3,4,5} | Katharina Wöran⁷ | Merima Herac⁷ | Judith Stift⁷ |
 Katharina Lampichler⁸ | Gerald Timelthaler⁹ | David Bauer^{1,2,6}  |
 Lukas Hartl^{1,2,6} | Bernhard Robl¹⁰ | Maria Sibila¹⁰ | Bruno K. Podesser¹¹ |
 Georg Oberhuber¹² | Philipp Schwabl^{1,2,3,4,5,6} | Mattias Mandorfer^{1,6}  |
 Michael Trauner¹ | Thomas Reiberger^{1,2,3,4,5,6} 

¹Division of Gastroenterology and Hepatology, Department of Internal Medicine III, Medical University of Vienna, Vienna, Austria

²Vienna Experimental Hepatic Hemodynamic Lab (HEPEX), Medical University of Vienna, Vienna, Austria

³Christian Doppler Laboratory for Portal Hypertension and Liver Fibrosis, Medical University of Vienna, Vienna, Austria

⁴Ludwig Boltzmann Institute for Rare and Undiagnosed Diseases, Vienna, Austria

⁵CeMM Research Center for Molecular Medicine of the Austrian Academy of Sciences, Vienna, Austria

⁶Vienna Hepatic Hemodynamic Laboratory, Division of Gastroenterology and Hepatology, Department of Medicine III, Medical University of Vienna, Vienna, Austria

⁷Department of Pathology, Medical University of Vienna, Vienna, Austria

⁸Department of Radiology and Nuclear Medicine, Medical University of Vienna, Vienna, Austria

⁹The Institute of Cancer Research, Department of Medicine I, Medical University of Vienna, Vienna, Austria

¹⁰Institute of Cancer Research, Department of Medicine I, Comprehensive Cancer Center, Medical University of Vienna, Vienna, Austria

¹¹Center for Biomedical Research, Medical University of Vienna, Vienna, Austria

¹²INNPATh, Institute of Pathology, University Hospital of Innsbruck, Innsbruck, Austria

Correspondence

Thomas Reiberger, Division of Gastroenterology and Hepatology, Department of Medicine III, Medical University of Vienna, Waehringer Guertel 18-20, A-1090 Vienna, Austria.
 Email: thomas.reiberger@meduniwien.ac.at

Funding information

Philipp Königshofer, Ksenia Brusilovskaya, Benedikt Simbrunner, Oleksandr Petrenko, Philipp Schwabl, and Thomas Reiberger were all cosponsored by the Austrian Federal Ministry for

Abstract

Background and Aims: Liver fibrosis is the static and main (70%-80%) component of portal hypertension (PH). We investigated dynamic components of PH by a three-dimensional analysis based on correlation of hepatic collagen proportionate area (CPA) with portal pressure (PP) in animals or HVPG in patients.

Approach and Results: Different animal models (bile duct ligation: $n = 31$, carbon tetrachloride: $n = 12$, thioacetamide: $n = 12$, choline-deficient high-fat

Abbreviations: 3D, three-dimensional; α -SMA, α -smooth muscle actin; ALD, alcohol-associated liver disease; BDL, bile duct ligation; BW, body weight; CCl₄, carbon tetrachloride; CDHFD, choline-deficient high-fat diet; CPA, collagen proportionate area; DAMP, damage-associated molecular pattern; HA, hyaluronic acid; HD-I, hyperdynamic index; HR, heart rate; IQR, interquartile range; MAP, mean arterial pressure; P3NP, procollagen type III N-terminal peptide; PBC, primary biliary cholangitis; PH, portal hypertension; PIGF, placental growth factor; PP, portal pressure; PSC, primary sclerosing cholangitis; PSR, picro-sirius red; SMABF, superior mesenteric artery blood flow; sVEGFR1, soluble vascular endothelial growth factor receptor 1; TAA, thioacetamide; TIMP1, tissue inhibitor of metalloproteinase 1; VCTE, vibration-controlled transient elastography; VWF-Ag, von Willebrand factor antigen.

This is an open access article under the terms of the Creative Commons Attribution-NonCommercial-NoDerivs License, which permits use and distribution in any medium, provided the original work is properly cited, the use is non-commercial and no modifications or adaptations are made.

© 2021 The Authors. *Hepatology* published by Wiley Periodicals LLC on behalf of American Association for the Study of Liver Diseases.

Digital and Economic Affairs, the National Foundation for Research, Technology and Development, Boehringer Ingelheim, and the Christian Doppler Research Association. Philipp Königshofer and Philipp Schwabl were supported by the Medical Scientific Fund of the Mayor of the City of Vienna (Project: 18070) awarded to Philipp Schwabl. Benedikt Simbrunner was supported by the International Liver Research Scholarship by Gilead Sciences awarded to Thomas Reiberger. Bernhard Robl and Maria Sibila were supported by an unrestricted grant from the European Research Council (ERC) advanced grant (ERC-2015-AdG TNT-Tumors 694883) granted to Maria Sibila

diet: $n = 12$) and patients with a confirmed single etiology of cholestatic (primary biliary cholangitis/primary sclerosing cholangitis: $n = 16$), alcohol-associated ($n = 22$), and metabolic (NASH: $n = 19$) liver disease underwent CPA quantification on liver specimens/biopsies. Based on CPA-to-PP/HVPG correlation, potential dynamic components were identified in subgroups of animals/patients with lower-than-expected and higher-than-expected PP/HVPG. Dynamic PH components were validated in a patient cohort ($n = 245$) using liver stiffness measurement (LSM) instead of CPA. CPA significantly correlated with PP in animal models ($Rho = 0.531$; $p < 0.001$) and HVPG in patients ($Rho = 0.439$; $p < 0.001$). Correlation of CPA with PP/HVPG varied across different animal models and etiologies in patients. In models, severity of hyperdynamic circulation and specific fibrosis pattern (portal fibrosis: $p = 0.02$; septa width: $p = 0.03$) were associated with PH severity. In patients, hyperdynamic circulation ($p = 0.04$), vascular dysfunction/angiogenesis (VWF-Ag: $p = 0.03$; soluble vascular endothelial growth factor receptor 1: $p = 0.03$), and bile acids ($p = 0.04$) were dynamic modulators of PH. The LSM-HVPG validation cohort confirmed these and also indicated IL-6 ($p = 0.008$) and hyaluronic acid (HA: $p < 0.001$) as dynamic PH components.

Conclusions: The relative contribution of “static” fibrosis on PH severity varies by type of liver injury. Next to hyperdynamic circulation, increased bile acids, VWF-Ag, IL-6, and HA seem to indicate a pronounced dynamic component of PH in patients.

INTRODUCTION

Chronic liver injury caused by miscellaneous etiologies leads to liver fibrosis and, ultimately, cirrhosis.^[1,2] Along with the progression of liver disease, necroinflammation and angiogenesis result in distortion of liver parenchymal architecture and remodeling of the hepatic vasculature.^[3] Consequently, intrahepatic vascular resistance increases, resulting in the development of portal hypertension (PH).^[4] Mechanistically, intrahepatic resistance is determined by “static” components (i.e., mainly fibrosis) and “dynamic” components (e.g., sinusoidal remodeling and abundance of vasoconstrictors).^[5] Fibrosis as the static component of PH represents the main determinant of intrahepatic resistance (70%-80%), whereas dynamic/vascular components may account for 20%-30%.^[6] In more advanced stages of PH, hyperdynamic circulation and increased splanchnic blood flow become a critical driver of PH.^[3]

Fibrosis evaluation was traditionally based on semiquantitative pathohistological scores on liver biopsy.^[7] Collagen is the main component of extracellular matrix in cirrhosis and, thus, the collagen proportionate area (CPA) is considered a valuable and objective biomarker of liver fibrosis severity.^[8-10] Automated determination

of CPA on liver histology by computer-assisted image analysis may be superior to semiquantitative histological scores for subclassifying cirrhosis^[11] and displays prognostic value toward hepatic decompensation and liver-related mortality in alcohol-associated liver disease (ALD).^[12] Furthermore, CPA correlated with clinical severity of cirrhosis and decompensation events in patients with HCV.^[13] Similarly, CPA displayed a stronger correlation to liver stiffness measured by vibration-controlled transient elastography (VCTE) than histological semiquantitative liver fibrosis staging.^[14] Previous studies in patients with HCV^[10] and ALD^[15] reported a correlation between CPA and HVPG. However, the diagnostic value of CPA remains to be evaluated for other liver diseases^[16] since fibrosis patterns profoundly differ by liver disease etiologies.^[17-20] As PH is a critical driver for complications in patients with advanced fibrosis,^[21,22] the potential correlation of CPA and PH severity is of clinical relevance. An accurate morphometric fibrosis assessment by histological CPA and its correlation to portal pressure (PP) will likely improve our understanding of the “static” and “dynamic” components of PH.

Thus, we aimed (i) to characterize the correlation of CPA with PP and HVPG in different animal models and different etiologies of human liver disease and (ii)

to identify potential dynamic modulators of PH based on a three-dimensional (3D) correlation model of CPA-to-PP/HVPG, respectively. Finally, we aimed (iii) to validate the dynamic modulators of PH in a noninvasive patient cohort using a VCTE-HVPG-based model.

MATERIAL AND METHODS

Animal models of liver fibrosis and PH

For this study, 114 male Sprague-Dawley rats (Him:OFA; 8-10 weeks old) were used in 4 different animal models (Figure 1A): the first model used surgical bile duct ligation (BDL; $n = 31$) to induce secondary biliary cirrhosis. The control group underwent a sham operation without ligation of the common bile duct (SHAM; $n = 11$). Toxic liver fibrosis was induced by repeated intraperitoneal injections of either carbon tetrachloride (CCl_4 ; $n = 12$) for 8 weeks (1 mL/kg 25% solution in olive oil; 3 \times /week), or thioacetamide (TAA; $n = 12$) for 12 weeks (150 mg/kg and dissolved in 0.9% saline; 3 \times /week). Control groups received olive oil (OO; $n = 12$) or saline (NaCl; $n = 12$) injections, respectively. NASH was induced by a model adapted from Nakamoto^[23] and Takayama^[24] using a choline-deficient high-fat diet (CDHFD; $n = 12$: HF-CDA, E15672-94, ssniff Spezialdiäten GmbH) for 12

weeks including intraperitoneal sodium nitrite injections as enhancer of liver fibrosis development for 7 weeks (25 mg/kg dissolved in PBS; 3 \times /week) starting at week 5 of the timeline. The control group was fed standard chow (CHOW; $n = 12$) and received PBS injections.

Hemodynamic readouts in animal models

Hemodynamic characterization of the portal hypertensive syndrome was performed by cannulation of the portal vein for PP measurement, by cannulation of the femoral artery for simultaneous measurement of heart rate (HR) and mean arterial pressure (MAP), and by measuring superior mesenteric artery blood flow (SMABF) using a perivascular ultrasound flow probe.^[25] The SMABF was adapted to body weight (BW) and the hyperdynamic index (HD-I) calculated by HR divided by MAP.

Patients

Patients undergoing HVPG measurements at the Hepatic Hemodynamic Laboratory of the Medical University of Vienna were included in this study. Inclusion criteria for analysis based on CPA/HVPG

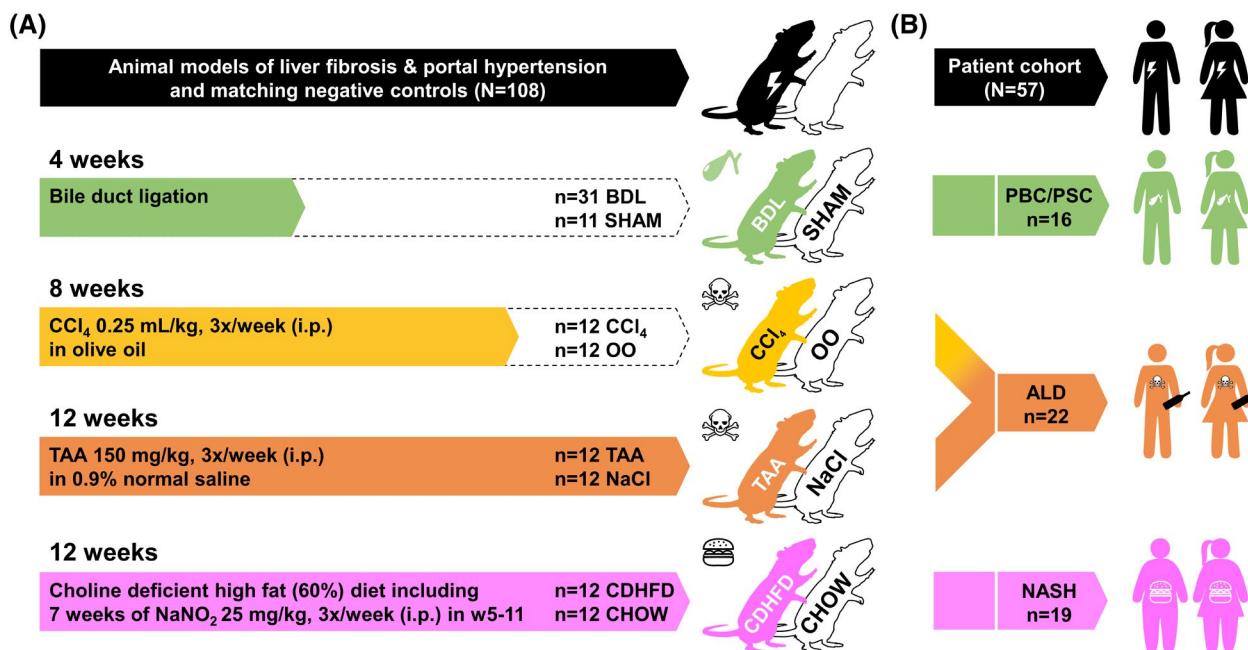


FIGURE 1 Experimental liver disease animal models and corresponding liver disease etiologies in patients. (A) BDL was performed to induce biliary cirrhosis for 4 weeks. The related control group underwent a sham operation (SHAM). Toxic liver fibrosis was induced by intraperitoneal injections of hepatotoxic CCl_4 for 8 weeks or TAA for 12 weeks, while control groups received only the related vehicle substances as injections: olive oil (OO) or isotonic saline (NaCl). NASH was induced by a combination of CDHFD for 12 weeks, including 7 weeks of intraperitoneal sodium nitrite (NaNO_2) injections. The control group was fed standard chow food (CHOW) and received injections of the vehicle substance for NaNO_2 : PBS. (B) Liver biopsies of 57 patients were classified as definite and single liver disease etiologies by pathologist: biliary liver diseases ($n = 16$: by PBC, PSC), ALD ($n = 22$), and NASH ($n = 19$)

correlation were (i) confirmed single/unequivocal etiology of liver disease, which corresponds to the etiologies of the animal models used, (ii) availability of liver biopsy within 6 month of the HVPG measurement, (iii) sufficient quality of the biopsy, and (iv) HVPG ≥ 6 mmHg, confirming the presence of PH. The second (validation) cohort using a model was based on the correlation of VCTE—an established surrogate of liver fibrosis severity^[26]—to HVPG included patients with (i) valid HVPG ≥ 6 mmHg and (ii) reliable VCTE assessment within 6 months of HVPG measurement.

HVPG, transjugular biopsy, and transient elastography

HVPG measurement including assessment of systemic hemodynamic parameters (i.e., HR, MAP, and HD-I) and liver biopsy were performed as previously described.^[27] VCTE (Fibroscan) was performed mainly at the same day of HVPG measurement.^[28]

Classification and affiliation of patients to liver disease etiology

Liver biopsies were stained with hematoxylin and eosin (Morphisto, Nr. 14580). Liver biopsies eligible for this study were reviewed for single etiologies of liver disease: primary biliary cholangitis (PBC), primary sclerosing cholangitis (PSC), ALD, or NASH (Figure 1B).

Morphometric analyses of CPA and pathohistological characterization of liver injury

Histological slides of animal liver specimens and human liver biopsies were stained with picro-sirius red (PSR; Morphisto, Nr. 13425). Slides were digitalized in high resolution of 40 \times magnification using a digital research slide scanner (Slideview VS200; OLYMPUS). Tissue was analyzed by quantitative morphometry software (HALO, V3.3.2541.184, Indica Labs) of PSR-stained area, which was considered as the percentage of CPA. Additionally, liver injury and fibrosis pattern—both in the animal and patient liver tissues—were comprehensively characterized by expert pathologists for distinct histopathological features: in this regard, the ISHAK score was used to stage fibrosis [F0-F6]; specific features of fibrosis patterns including perivenular, periportal, and portal fibrosis; the width of fibrotic septa; ductular proliferation; and bile duct damage; and all were evaluated using a semiquantitative score [0-3].

Correlation of CPA-to-PP/HVPG and subsequent stratification into a 3D model

CPA levels were correlated to PP in animals and HVPG in patients, followed by the evaluation of the correlation of CPA-to-PP/HVPG in each subgroup of liver injury or liver disease etiology, respectively. For further analyses, the animal data set was reduced to diseased animals to facilitate comparison to patient data. Based on the linear regression models in the animal and the patient cohort, data points within the interquartile range (IQR) were considered as animals/patients with expected PP/HVPG by CPA (~PP/HVPG). In contrast, data points below and above the IQR of the linear regression model were considered as animals/patients with lower-than-expected PP/HVPG (-PP/HVPG) and higher-than-expected PP/HVPG (+PP/HVPG) (Figure 4A).

Analysis of potential dynamic components of PH

Different dynamic components of PH were analyzed by assessing differences of biomarkers/surrogates between animals of -/~/+PP or patients of -/~/+HVPG. In diseased animals, organ-to-BW ratios of liver and spleen, the laboratory parameters bilirubin and aminotransferases (aspartate aminotransferases and alanine aminotransferases), and systemic hemodynamic parameters (e.g., HR, MAP, HD-I, and SMABF) were analyzed. In patients, laboratory and systemic hemodynamic parameters analog to animal models (except of SMABF) were investigated and extended for additional biomarkers/surrogates: bile acid level, IL-6, von Willebrand factor antigen (VWF-Ag), placental growth factor (PIGF), soluble vascular endothelial growth factor receptor 1 (sVEGFR1), the PIGF/sVEGFR1 ratio, Enhanced Liver Fibrosis score and its single components: tissue inhibitor of metalloproteinase 1 (TIMP1), procollagen type III N-terminal peptide (P3NP) and hyaluronic acid (HA). Access to imaging data enabled analysis on presence of collaterals, spleen diameter, and spleen volume. Certain pathohistological features were also included into analysis. Immunohistochemistry stainings for α -smooth muscle actin (α -SMA) and CD31 (platelet endothelial cell adhesion molecule) as surrogate markers for hepatic stellate cell activation/contraction and for (sinusoidal) endothelial dysfunction, respectively, were considered whenever available from sufficient biopsy material.

Statistical analyses

Results were presented as mean \pm SEM or median and IQR as appropriate by the distribution of the respective parameters. Correlation coefficients (Rho)

were calculated by Spearman's correlation. *t* test with Welch's correction or Mann-Whitney test were used for comparison to healthy controls. One-way ANOVA test and Tukey's multiple comparison correction or Kruskal-Wallis test and Dunn's multiple comparison correction were used for group comparisons between the etiologies and the stratified groups of $-/+PP/HVPG$ as predicted by CPA. GraphPad Prism (v9.0, GraphPad Software) was used for all analyses, and a two-sided *p* value ≤ 0.05 was defined to denote statistical significance.

RESULTS

Characteristics of the different animal models and patient cohorts

Characteristics of the diseased animals including 31 BDL (46%), 12 CCl_4 (18%), 12 TAA (18%), and 12 CDHFD rats (18%) are summarized in Supporting Table ST-1. The characteristics of the 57 patients used for the primary CPA/HVPG correlation analysis included 16 patients with PSC/PBC (28%), 22 with ALD (39%), and 19 with NASH (33%) are summarized in Supporting Table ST-2. The data from their CPA-HVPG correlation analysis was subsequently used to build the 3D model for the identification of potential dynamic modulators of PH severity. Finally, another cohort of $n = 245$ patients was included for assessing the VCTE/HVPG correlation and validation of the surrogate markers of dynamic PH components. The liver disease etiologies in patients of the validation cohort were PBC/PSC (7%), ALD (47%), NASH (6%), viral hepatitis (19%), mixed etiology (6%), and cryptogenic liver disease (15%), and their characteristics are summarized in Supporting Table ST-3.

The correlation of CPA with PP in animal models varies by type of liver injury

CPA significantly correlated with PP in the overall cohort of animals including healthy controls ($n = 114$; $Rho = 0.830$, $p < 0.001$; see Supporting Figure SF-1). Individually analyzed by type of model, the linear correlation of CPA-to-PP was still significant ($p < 0.001$) but varied in strength and even more importantly by the slope (i.e., the linear regression coefficient) across the different models.

Considering only diseased animals, there was still a strong and significant correlation ($n = 67$; $Rho = 0.531$; $p < 0.001$; Figure 2) of CPA to PP. Within the respective models, the correlation of CPA-to-PP was strong in the CCl_4 ($Rho = 0.643$; $p = 0.03$) and in the CDHFD animals ($Rho = 0.616$; $p = 0.04$) but nonsignificant in the TAA and BDL models. Both toxic models (CCl_4 and

TAA) showed a similar slope of the CPA-PP correlation line. Importantly, in the BDL animals, higher PP values were already seen at the lower CPA levels, as compared with all other models' fitting lines, and thus generally stand out from the correlation data compared with other models.

The semiquantitative assessment of different histopathologic features varied across the different animal models with significantly increased ISHAK score in TAA animals compared with all other models: $p < 0.001$ versus BDL, $p < 0.001$ versus CCl_4 , and $p = 0.01$ versus CDHFD animals. Perivenular fibrosis showed significantly decreased presence in TAA animals ($p = 0.04$ vs. BDL), and BDL animals showed significant increased presence of periportal fibrosis against CCl_4 ($p < 0.001$), TAA ($p < 0.001$) and CDHFD animals ($p = 0.007$). Portal fibrosis and septa width showed significantly reduced presence in CCl_4 and CDHFD animals ($p < 0.001$ vs. BDL&TAA). Histopathologic features of ductular proliferation ($p < 0.001$ vs. CCl_4 , $p = 0.007$ vs. TAA, $p < 0.001$ vs. CDHFD) and bile duct damage ($p = 0.002$ vs. CCl_4 , $p = 0.002$ vs. TAA, $p = 0.002$ vs. CDHFD) were significantly higher scored in BDL models compared with all other models. Thereby, the BDL model exhibited distinct differences in terms of more advanced periportal fibrosis, ductular proliferation, and bile duct damage.

Although the diseased models differed in fibrosis severity (i.e., in CPA%), the expert pathologist examination confirmed important histopathological features that reflect their corresponding human liver disease etiology—to be present in the included models. A detailed and comprehensive overview on all evaluated characteristics, including CPA, PH severity, and distinct pathohistological features of all animal models are summarized in the Supporting Information (Supporting Figure SF-2A, Supporting Tables ST-4A, ST-5A, and ST-6).

The correlation of CPA with HVPG varies by human liver disease etiology

CPA significantly correlated with HVPG in the overall patient cohort ($n = 57$; $Rho = 0.439$; $p < 0.001$). When different etiologies were separately analyzed, the correlation of CPA-to-HVPG was significant in patients with ALD ($Rho = 0.464$, $p = 0.03$) and NASH ($Rho = 0.544$, $p = 0.02$). Interestingly, within the cholestatic etiologies of patients with PBC/PSC, the correlation of CPA-to-HVPG was no longer significant ($p = 0.73$). Patients with PBC/PSC (similar to BDL animals) yield higher HVPG levels at lower CPA values, as evident from the etiology-dependent linear fitting curves (Supporting Table ST-4B). In addition to differences in the CPA-to-HVPG correlations, the different human liver disease etiologies were associated with

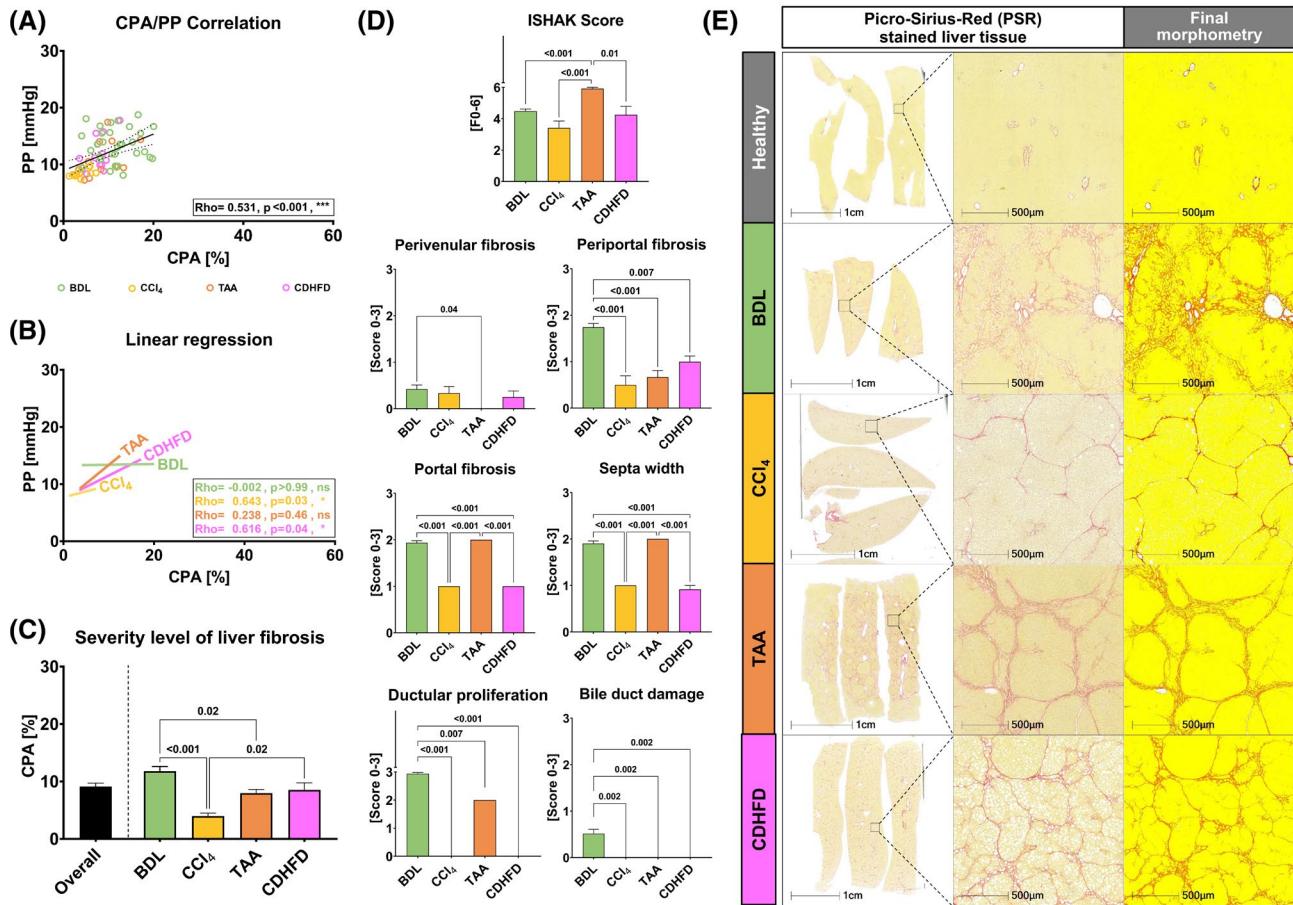


FIGURE 2 Histologic assessments and hemodynamic correlations in different animal models of liver disease. Overall, $n = 67$ diseased animals were studied (BDL: $n = 31$, CCl₄: $n = 12$, TAA: $n = 12$, CDHFD: $n = 12$). (A) Correlation of CPA with PP. (B) Correlations of CPA-to-PP are shown separately for the different animal models as linear regression lines. (C) Comparison of diseased animal models by severity level of liver fibrosis shown by CPA%. (D) Comprehensive histologic characterization of each model by ISHAK score and different pathologic features including perivascular, periportal, and portal fibrosis, septa width, ductular proliferation, and bile duct damage semiquantitatively scored by 0-3. (E) Representative histological images of PSR-stained liver tissue are shown, including the final morphometry analysis performed on whole liver lobe slide scans. (Significant p values are stated within each graph. Statistical tests used: one-way ANOVA test and Tukey's multiple comparison correction or Kruskal-Wallis test and Dunn's multiple comparison correction)

distinct histopathologic features that largely varied across etiologies (Figure 3).

The severity level of liver fibrosis (defined by CPA%) was not different but was comparable across the patients in the different liver disease etiologies. The patients with PBC/PSC showed significant differences in perivascular fibrosis (<0.001) as compared with ALD and in bile duct damage as compared with ALD ($p = 0.02$) and NASH ($p = 0.03$). Detailed information on statistical comparison of CPA and PH severity between etiologies are summarized in the Supporting Information (Supporting Figure SF-2B, Supporting Tables ST-5B and ST-7).

Assessment of dynamic components of PH in animal models of liver disease

Based on the linear regression model of CPA-to-PP, animals outside the IQR (\sim PP, $n = 37$) correlation

were grouped in animals of lower-than-expected ($-$ PP, $n = 16$) and higher-than-expected ($+$ PP, $n = 14$) PP (Figure 4B). Parameters with significant differences among these groups and nonsignificant but clear increasing/decreasing trends across animals of $-/\sim/+$ PP are highlighted in Figure 4F. The toxic models of CCl₄ and TAA animals were combined to one united group corresponding to human ALD etiology. The proportion of the different models ("etiologies") across the groups of $-$ PP vs. $+$ PP was rather similar (Figure 4C). Detailed characteristics and comparison results of $-/\sim/+$ PP groups are summarized in Supporting Table ST-8.

The impact of hyperdynamic circulation as an important dynamic component of PH in animal models was suggested by the increasing splanchnic blood flow (upward trend of SMABF/BW across the groups of $-/\sim/+$ PP). Animals with $+$ PP had significantly increased liver/BW ratios ($p = 0.01$), and more pronounced portal

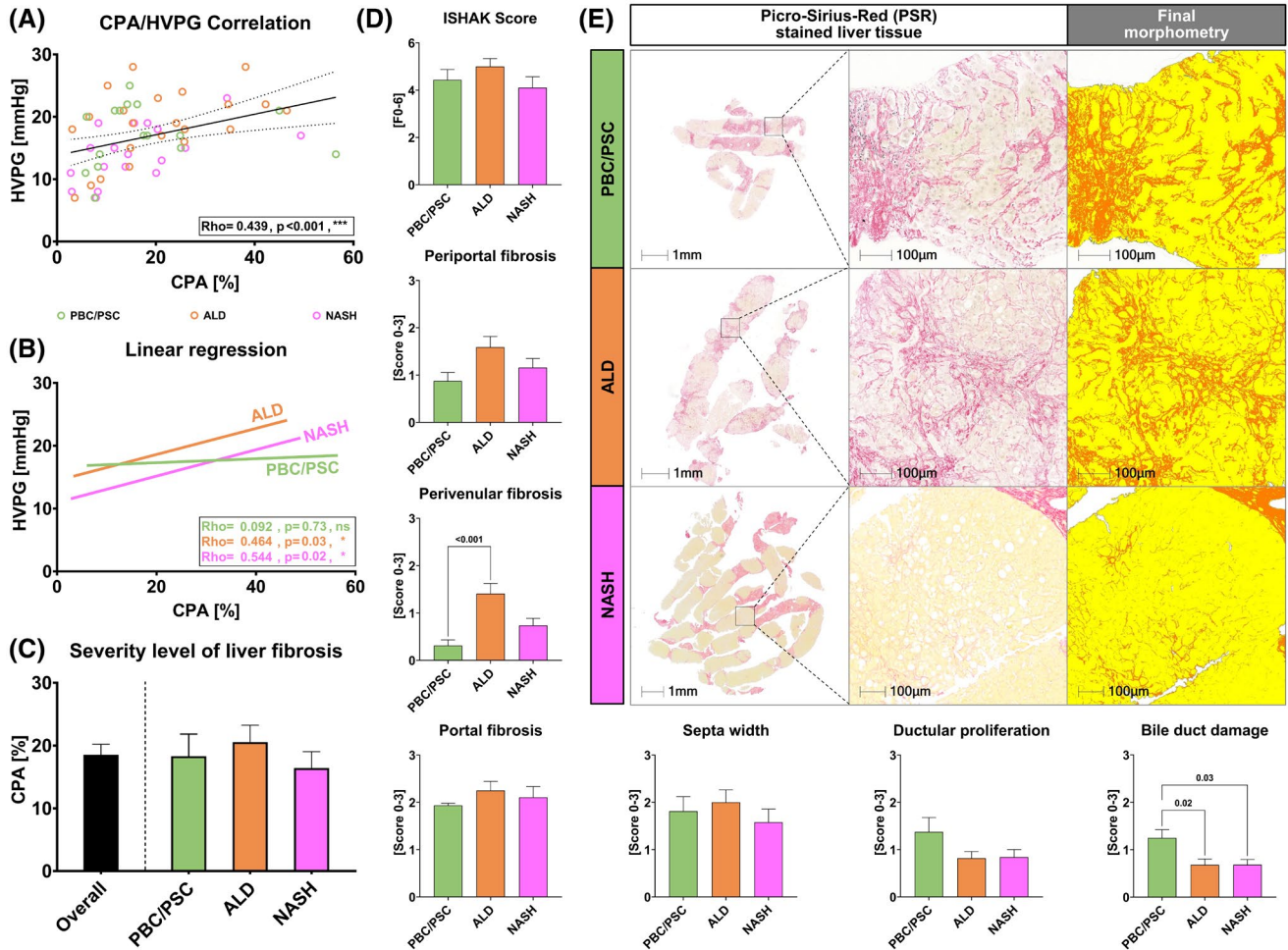


FIGURE 3 Histologic assessment and hemodynamic correlation in patients with different liver disease etiologies. Overall, $n = 57$ patients were included: $n = 16$ with PBC/PSC, $n = 22$ with ALD, and $n = 19$ with NASH. (A) Correlation of CPA with HVPG. (B) Correlations of CPA-to-HVPG are shown separately for different groups/etiologies of human liver disease as linear regression lines. (C) Comparison of liver fibrosis severity (CPA%) between the different human liver disease groups. (D) Comprehensive characterization of each etiology group by ISHAK score and histopathologic features: perivenular, periportal, and portal fibrosis, septa width, ductular proliferation, and bile duct damage scored by 0-3. (E) Representative histological images of PSR-stained liver biopsies, including the final morphometry analysis performed on the whole biopsy slide scans. (Significant p value stated within each graph. Statistical tests used: one-way ANOVA test and Tukey's multiple comparison correction or Kruskal-Wallis test and Dunn's multiple comparison correction)

fibrosis ($p = 0.03$) and septa width ($p = 0.02$) vs. animals of $-PP$. Ductular proliferation and bile duct damage was also more pronounced in animals with $+PP$, as underlined by the systematic upward trend of the respective histological semiquantitative scores for ductular proliferation and bile duct damage across animals of $-/+PP$.

Assessment of dynamic components of PH in patients

Stratification of patients into those with $-HVPG$ ($n = 12$), $\sim HVPG$ ($n = 30$), and $+HVPG$ ($n = 15$) was performed similarly to animals (Figure 4D). The proportion of different liver disease etiologies (PBC&PSC/ALD/NASH)

was almost equal across the estimated HVPG groups with 25/33/42% in $-HVPG$, 23/33/43% in $\sim HVPG$, and 25/33/42% in $+HVPG$ (Figure 4E). Detailed characteristics and statistical comparisons of the $-/+HVPG$ groups are summarized in Supporting Table ST-9. Differences of surrogate biomarkers of dynamic components of PH across patients of $-/+HVPG$ are highlighted in Figure 5.

Hyperdynamic circulation was identified as modulator of PH by significantly increased HD-I in patients with $+HVPG$ ($p = 0.04$) vs. $-HVPG$. The important role of hyperdynamic circulation was confirmed by a clear trend of increasing spleen diameter from patients of $-HVPG$ to $+HVPG$, suggesting a splanchnic hyperperfusion component of PH. VWF-Ag levels as marker for vascular dysfunction were significantly increased in patients

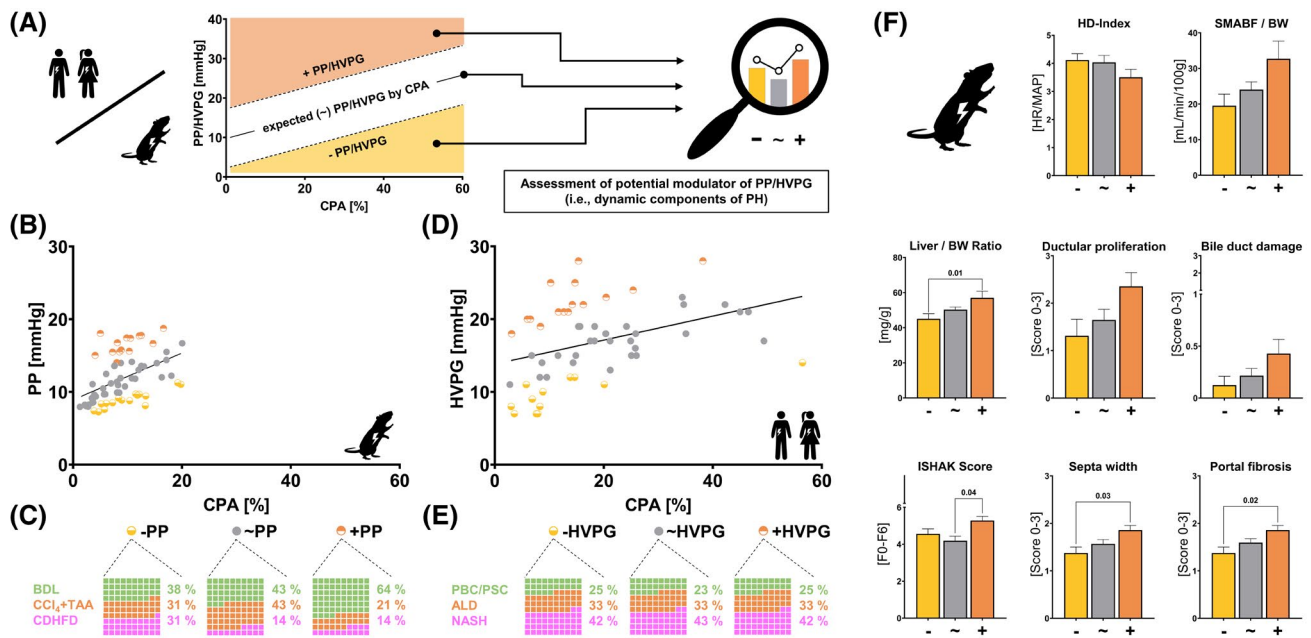


FIGURE 4 Identification of potential modulators of PH: (A) 3D analysis model by stratification of dataset into groups of lower-than-expected (-PP/HVPG), expected (~PP/HVPG, inside the IQR), and higher-than-expected (+PP/HVPG) PP or HVPG as predicted from the linear regression model based on histological fibrosis area (CPA%). (B) Visualized allocation of study cohort into animals of -/~+/+PP ($n = 16/37/14$) and (C) proportion of different animal models represented in each group. (D) Visualized allocation of the study cohort into patients of -/~+/+HVPG ($n = 12/30/15$) and (E) proportion of human liver disease etiologies represented in each group. (F) Potential modulators of PH were identified by statistical significance or a logic trend across the different groups of animals with -PP vs. ~PP vs. +PP, respectively

with +HVPG vs. ~HVPG ($p = 0.03$). sVEGFR1 levels as a biomarker for pathologic angiogenesis was significantly increased in patients with -HVPG vs. ~HVPG ($p = 0.03$), suggesting angiogenesis-driven collateralization as a protective factor in PH. Bile acid levels were significantly elevated in patients with +HVPG vs. ~HVPG ($p = 0.04$). In addition, there was an uprising trend of bile duct damage and ductular proliferation from patients with -HVPG to +HVPG. In regard to pathohistologic features, periportal, and portal fibrosis and septa width showed a similar uprising trend across patients of -/~+/+HVPG. In the CPA-HVPG cohort, there were only trends toward higher levels of the inflammation marker IL-6 and the matrix turnover makers TIMP1, P3NP, and HA. Hepatic stellate cell activation/contraction, as suggested by a higher histologic α -SMA expression, showed a strong and significant correlation to severity of liver fibrosis (CPA%). However, a clear α -SMA-driven dynamic component was not evident across -HVPG to +HVPG groups. In contrast, CD31—as a marker of sinusoidal capillarization—was clearly increasing in patients of +HVPG while being lower in patients of -HVPG and intermediate expression in patients with ~HVPG. However, CD31 expression (capillarization) was not associated with histologic fibrosis severity (CPA%), suggesting it may occur independently from static fibrosis and thus modulate intrahepatic vascular resistance as a dynamic component of PH.

Validation of dynamic modulators of PH in the VCTE-HVPG cohort

Using a larger validation cohort undergoing VCTE-based fibrosis assessment ($n = 245$), the correlation of liver stiffness measurement-based fibrosis to HVPG remained highly significant ($Rho = 0.638$, $p < 0.001$), and the regression model fitting line was similar to the CPA-HVPG model. Figure 6 shows stratification of patients into groups of -/~+/+HVPG ($n = 65/122/58$) based on the IQR of the VCTE/HVPG correlation. Detailed patient characteristics and statistical comparisons of -/~+/+HVPG groups are summarized in the Supporting Information (Supporting Tables ST-10, ST-11, ST-12, ST-13; Supporting Figures SF-3[I] and SF-3[II]).

In summary, the VCTE-HVPG correlation data confirmed the significant impact of hyperdynamic circulation (HD-I, spleen diameter), cholestasis (i.e., bile acid levels), and sinusoidal/endothelial dysfunction (VWF-Ag) as critical dynamic modulators of PH. In addition, some trends in the CPA-HVPG cohort showing an impact of systemic inflammation, and matrix remodeling markers on the dynamic component of PH were confirmed in the VCTE-HVPG validation cohort: specifically, IL-6 levels were significantly lower in patients with lower-than-expected HVPG ($p = 0.008$), suggesting that a low level of inflammation allows for dynamic compensation of PH. Furthermore, the HA—an important damage-associated

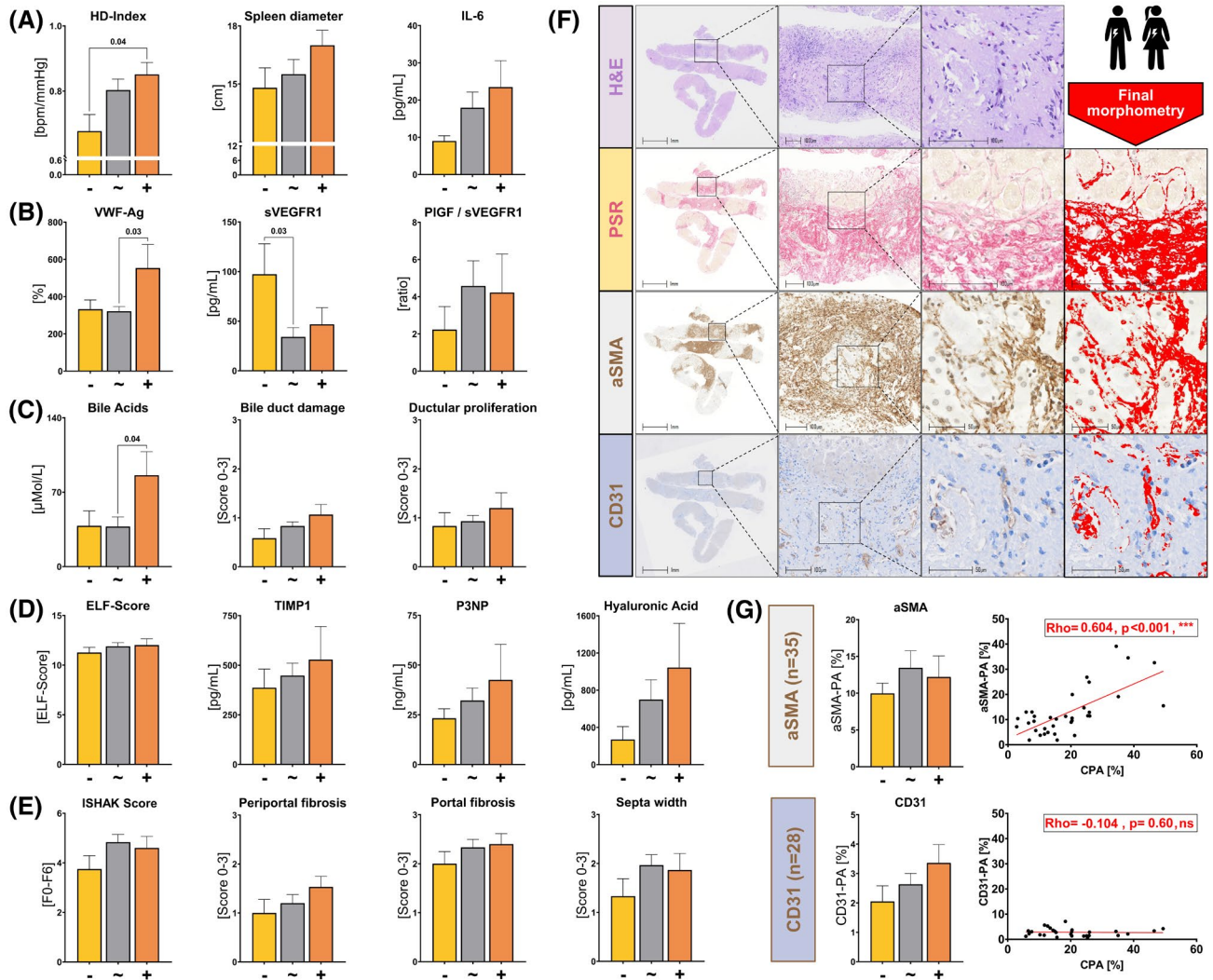


FIGURE 5 Identification of potential modulators of PH in patients according to lower vs. higher-than-expected HVPG (-/+HVPG, $n = 12/15$) vs. the IQR (~HVPG, $n = 30$). (A) HD-I (HR/MAP), spleen diameter, and the systemic inflammation biomarker IL-6. (B) VWF-Ag levels as marker for endothelial dysfunction and the angiogenesis marker sVEGFR1 and its ratio to PIGF. (C) Bile acid level and histopathological bile duct damage and ductular proliferation as indicators of biliary damage. (D) Enhanced Liver Fibrosis (ELF) score and its single components TIMP1, P3NP, and HA. (E) Additional pathohistologic liver fibrosis features as ISHAK score, periportal and portal fibrosis, and septa width. (F) Representative histological images of hematoxylin and eosin (H&E), PSR, α -SMA, and CD31-stained liver tissue, including the final morphometry analysis performed on the whole slide scans. (G) Histologic α -SMA and CD31 expression pattern across -/+HVPG and their correlation of each parameter to respective CPA data

molecular pattern (DAMP)—was significantly more elevated in patients with higher-than-expected HVPG than in patients with lower-than-expected HVPG ($p < 0.001$).

DISCUSSION

PH is determined by a static intrahepatic (70%-80%) and dynamic (20%-30%) components of intrahepatic resistance and hyperdynamic (splanchnic) circulation. However, the exact molecular drivers of the dynamic PH component—which might be different across liver disease etiologies—have not been deciphered in detail. In this study, we investigated potential modulators of PH by subgroup stratification based on a CPA-regression

model into animal/patient groups with lower-than-expected versus higher-than-expected PH severity.

Liver fibrosis as the static component of PH was traditionally evaluated on liver biopsy by semiquantitative pathological scores; however, fibrosis quantification by CPA seems superior due to a higher linear range and a lower risk for interobserver variability.^[8-10] Due to the high contrast, PSR staining was most commonly used for automated morphometric analysis of CPA. In our study, PSR-based CPA correlated significantly with PP in animals and with HVPG in patients. Importantly, while previous studies showed good correlations of CPA-to-HVPG in patients with HCV^[10] and nonabstinent patients with ALD,^[15] our study now extends these findings to patients with NASH. In the cholestatic

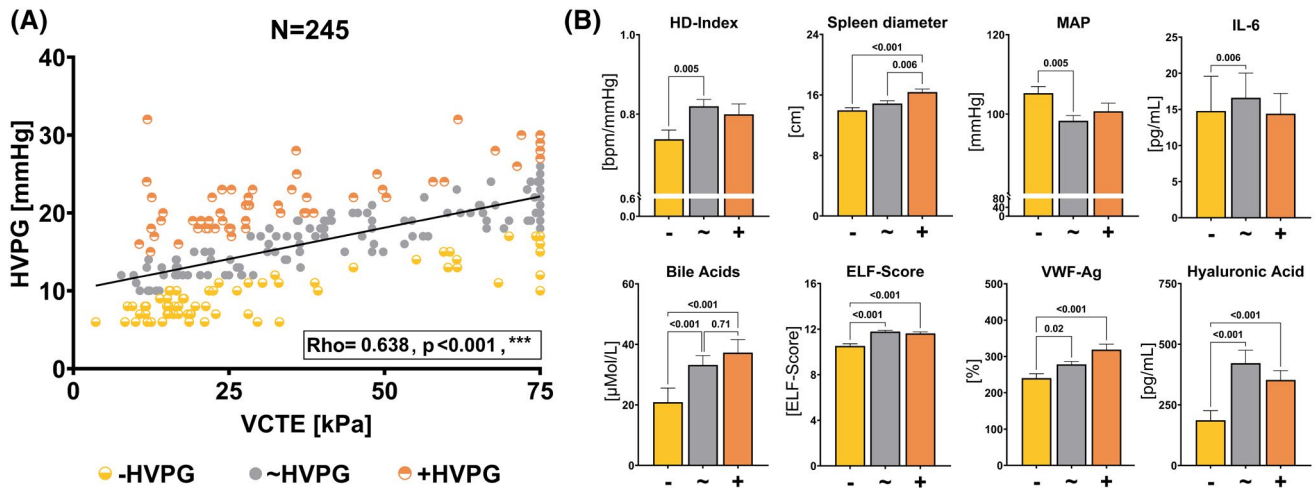


FIGURE 6 (A) Visualized allocation of patients with $-/\sim/+$ HVPG by stratification ($n = 65/122/58$) based on the correlation of VCTE with HVPG in another patient cohort including various etiologies of liver disease ($n = 245$). (B) Identification of potential dynamic modulators of PH across patient groups of $-/\sim/+$ HVPG

etiologies PBC and PSC, however, the CPA was less well correlated with HVPG, indicating distinct pathomechanisms to be involved in PH development in these liver disease etiologies. Interestingly, both patients with PBC and patients with PSC had highest values of HVPG at lower CPA values and showed more pronounced ductular proliferation and periportal fibrosis as distinct histopathologic features, which suggest a presinusoidal component of PH that occurs in early PBC/PSC disease (i.e., early fibrosis) stages.

Using standardized and well-established animal models of different types of liver injury next to patient data, we demonstrate an etiology-dependent correlation of CPA-to-PP/HVPG. These significant correlations of CPA to PP in liver-diseased animals and to HVPG in patients enabled subsequent assessment of potential dynamic PH components by a 3D regression model.

In patients with +HVPG, a significantly higher HD-I (higher HR, lower MAP) was found, suggesting a critical contribution of hyperdynamic circulation to severe PH, which was also confirmed by the cohort of patients with VCTE/HVPG. Importantly, the animal data showed an increased splanchnic blood flow (SMABF/BW) across animals of $-/\sim/+$ PP, which again demonstrates increased portal blood inflow as dynamic component of PH,^[29,30] which can, however, be targeted by nonselective betablockers.^[31,32]

The extent of portosystemic collaterals did not differ between all analyzed groups; however, pathological angiogenesis still seems to impact PH severity because patients with -HVPG showed a lower PIGF/sVEGFR1 ratio due to significantly increased sVEGFR1 levels. Mechanistically, sVEGFR1 may trap PIGF and thereby limit the bioavailability of PIGF and inhibit angiogenesis,^[33,34] resulting in higher PIGF/sVEGR1 ratios in patients with more pronounced PH (i.e., in patients with $+/\sim$ -HVPG).

Sinusoidal endothelial dysfunction has been proposed as a major factor contributing to intrahepatic vascular resistance. The (sinusoidal) endothelium-derived VWF-Ag represents a promising soluble biomarker in cirrhosis, and also, in our study, we found significantly elevated VWF-Ag values in patients with +HVPG (both in the VCTE and CPA cohort) as compared with patients with ~HVPG. Accordingly, VWF-Ag levels were lower in patients with less pronounced PH (-HVPG). Taken together, VWF-Ag as a soluble biomarker of (sinusoidal) endothelial dysfunction, reflecting the important contribution of intrahepatic sinusoidal vascular resistance^[35-37] as a dynamic component of PH.

Next, bile acids were identified as modulator of PH severity, with increasing levels across patients with $-/\sim/+$ HVPG (both in the CPA-HVPG and VCTE-HVPG cohort). Both BDL animals and patients with PBC/PSC exhibited distinct histopathologic features of ductular proliferation and bile duct damage. These features together with pronounced periportal fibrosis may explain the aberrant correlation fitting curve of CPA with PP/HVPG resulting from a strong presinusoidal component of PH caused by fibrosis around portal vein branches that critically determines vascular resistance. However, these hypotheses require further confirmation. Still, cholestasis—as observed in the BDL models and patients with PBC/PSC—seems to increase the dynamic PH, which may be related to vasoactive effects of bile acids.^[38,39]

Hepatic inflammation may also contribute as a dynamic component to PH. IL-6 represents a proinflammatory biomarker in patients with cirrhosis.^[40] In the CPA-HVPG cohort, IL-6 levels demonstrated a clear uprising (but nonsignificant) trend across the patient groups of $-/\sim/+$ HVPG. In the VCTE-HVPG validation cohort, significantly decreased levels of IL-6 were shown in patients with lower severity of PH (i.e., the

–HVPG group). Overall, these findings affirm that a proinflammatory state is associated with increased intrahepatic resistance,^[41] and thus, IL-6 might be used as a surrogate for a pronounced dynamic component of PH.

Finally, the DAMP HA showed a clear uprising trend across the groups of patients with –/+HVPG, with the highest levels observed in patients with pronounced PH (i.e., the +HVPG group). This suggested that ongoing liver injury and active fibrogenesis associate with pathologic sinusoidal resistance as a critical dynamic component of PH. The role of HA as a dynamic modulator of PH was confirmed in the VCTE-HVPG validation cohort.

Our study has several limitations: In the animal models, we have to acknowledge that the hemodynamic assessment of PP had to be performed under general anesthesia. In addition, the fibrosis severity was different across the included animal models. Moreover, animal models never reflect all features of the corresponding human liver disease that develops mostly over years as opposed to a typical model duration of just a few weeks. The BDL model represents an artificial surgically induced cholestatic model that does not mimic important features of human PBC or PSC. Many animal models of ALD do not show significant fibrosis or PH, which is why we only used CCl₄ and TAA models that exhibit both pronounced fibrosis and PH. Finally, a perfect NASH animal model that shows all features of human NASH is hitherto not available.

In patients, it has to be acknowledged that HVPG does not capture the presinusoidal components of PH, which might be of particular relevance in NASH^[42] or PBC.^[43] Another limitation of our study includes the small sample size in the cohort of patients with CPA-HVPG. However, this was partly due to a strict selection strategy, which in turn guaranteed a very clean dataset and allowed more confidence in the statistical findings.

In conclusion, our data provide important insights on the interaction of fibrosis quantity and quality across different types and etiologies of liver injury with PH severity. Importantly, we specifically established hyperdynamic (splanchnic) circulation, bile acids, sVEGFR1, VWF-Ag, IL-6, and the DAMP HA as critical dynamic modulators of PH. Furthermore, we recommend automated morphometric fibrosis assessment for accurate quantification of fibrosis, which allows for an improved understanding of the structural hepatic components of PH in future studies. As a future perspective, the identification of patients with more pronounced dynamic components of PH may particularly benefit from therapies targeting the hyperdynamic (splanchnic) circulation, systemic inflammation, and molecular pathways related to cholestasis and sinusoidal endothelial remodeling.

ACKNOWLEDGMENTS

The financial cosupport by the Austrian Federal Ministry for Digital and Economic Affairs, the National

Foundation for Research, Technology and Development, the Christian Doppler Research Association, and Boehringer is gratefully acknowledged.

CONFLICT OF INTEREST

Philipp Königshofer, Ksenia Brusilovskaya, Benedikt Simbrunner, Oleksandr Petrenko, Philipp Schwabl, Thomas Reiberger were all co-supported by the Austrian Federal Ministry for Digital and Economic Affairs, the National Foundation for Research, Technology and Development, Boehringer Ingelheim, and the Christian Doppler Research Association. Philipp Schwabl received speaking honoraria from Bristol-Myers Squibb, and Boehringer-Ingelheim, consulting fees from PharmaIN, and travel support from Falk and Phenex Pharmaceuticals. Benedikt Simbrunner received travel support from AbbVie and Gilead and was supported by the International Liver Research Scholarship by Gilead Sciences awarded to Thomas Reiberger. Thomas Reiberger received grant support from Abbvie, Boehringer-Ingelheim, Gilead, MSD, Philips Healthcare, Gore; speaking honoraria from Abbvie, Gilead, Gore, Intercept, Roche, MSD; consulting/advisory board fee from Abbvie, Bayer, Boehringer-Ingelheim, Gilead, Intercept, MSD, Siemens; and travel support from Abbvie, Boehringer-Ingelheim, Gilead and Roche. Judith Stift received grant support from Gilead, Eli, and Lilly. David Bauer has received travel support by Gilead and AbbVie and speaker fees from AbbVie. Mattias Mandorfer served as a speaker and/or consultant and/or advisory board member for AbbVie, Bristol-Myers Squibb, Gilead, Collective Acumen, and W. L. Gore & Associates and received travel support from AbbVie, Bristol-Myers Squibb, and Gilead. Michael Trauner has received research grants from Albireo, Cymabay, Falk, Gilead, Intercept, MSD and Takeda and travel grants from Abbvie, Falk, Gilead and Intercept. He further has advised for Albireo, BiomX, Boehringer Ingelheim, Falk Pharma GmbH, Genfit, Gilead, Intercept, Janssen, MSD, Novartis, Phenex, Regulus and Shire and has served as speaker for Falk Foundation, Gilead, Intercept and MSD. He is also co-inventor of patents on the medical use of NorUDCA filed by the Medical Universities of Graz and Vienna. Katharina Wöran, Katharina Lampichler, Gerald Timelthaler, Bruno K. Podesser, Georg Oberhuber, Lukas Hartl, Maria Sibilia, Merima Herak, and Bernhard Robl declare no conflict of interest.

ETHICS

Procedures involving animal subjects have been approved by the animal ethics committee of the respective Austrian Government by identification numbers BMWFW-66.009/0345-WF/V/3b/2014, BMWFW-66.009/0245-WF/V/3b/2016, and BMBWF-66009-0097-V-3b-2018. All experiments were performed in accordance with the guidelines of the Laboratory Animal Care and Use Committee (ACUC) of the Medical


University of Vienna, Animal Research: Reporting of In Vivo Experiments (ARRIVE) guidelines, next to the 3Rs^[44] and FELASA guidelines.^[45] The patients and their biospecimens included/used in this analysis were recruited from clinical studies approved by the local Ethics Committee (EK 1262/2017, EK 1697/2017, and EK 2318/2019) and the study was conducted in accordance with the principles of the Declaration of Helsinki. Written informed consent was obtained from all patients and no donor organs were obtained from executed prisoners or other institutionalized persons.

AUTHOR CONTRIBUTIONS

Data collection: Philipp Königshofer, Benedikt Silvester Hofer, Ksenia Brusilovskaya, Benedikt Simbrunner, Oleksandr Petrenko, Katharina Wöran, Merima Herac, Judith Stift, Katharina Lampichler, Gerald Timelthaler, David Bauer, Lukas Hartl, Bernhard Robl, Georg Oberhuber, Philipp Schwabl, Mattias Mandorfer, and Thomas Reiberger. **Statistical analysis:** Philipp Königshofer, Benedikt Silvester Hofer, and Thomas Reiberger. **Drafting of the manuscript:** Philipp Königshofer and Thomas Reiberger. **Study supervision:** Philipp Schwabl, Mattias Mandorfer, Michael Trauner, and Thomas Reiberger. **Revision for important intellectual content and approval of the final version of the manuscript:** Philipp Königshofer, Benedikt Silvester Hofer, Ksenia Brusilovskaya, Benedikt Simbrunner, Oleksandr Petrenko, Katharina Wöran, Merima Herac, Judith Stift, Katharina Lampichler, Gerald Timelthaler, David Bauer, Lukas Hartl, Bernhard Robl, Maria Sibila, Bruno K. Podesser, Georg Oberhuber, Philipp Schwabl, Mattias Mandorfer, Michael Trauner, and Thomas Reiberger.

ORCID

Philipp Königshofer  <https://orcid.org/0000-0003-1279-1148>

Benedikt Simbrunner  <https://orcid.org/0000-0001-8181-9146>

David Bauer  <https://orcid.org/0000-0002-9363-8518>

Mattias Mandorfer  <https://orcid.org/0000-0003-2330-0017>

Thomas Reiberger  <https://orcid.org/0000-0002-4590-3583>

REFERENCES

- Tsochatzis EA, Bosch J, Burroughs AK. Liver cirrhosis. *Lancet*. 2014;383(9930):1749–61.
- Hernandez-Gea V, Friedman SL. Pathogenesis of liver fibrosis. *Annu Rev Pathol*. 2011;6(1):425–56.
- Iwakiri Y. Pathophysiology of portal hypertension. *Clin Liver Dis*. 2014;18(2):281–91.
- Reiberger T, Mandorfer M. Beta adrenergic blockade and decompensated cirrhosis. *J Hepatol*. 2017;66(4):849–59.
- Bhathal PS, Grossman HJ. Reduction of the increased portal vascular resistance of the isolated perfused cirrhotic rat liver by vasodilators. *J Hepatol*. 1985;1(4):325–37.
- Bosch J, Groszmann RJ, Shah VH. Evolution in the understanding of the pathophysiological basis of portal hypertension: How changes in paradigm are leading to successful new treatments. *J Hepatol*. 2015;62(1):S121–S130.
- Pinzani M, Rombouts K, Colagrande S. Fibrosis in chronic liver diseases: diagnosis and management. *J Hepatol*. 2005;42(Suppl 1):S22–S36.
- Buzzetti E, Hall A, Ekstedt M, Manuguerra R, Guerrero Misas M, Covelli C, et al. Collagen proportionate area is an independent predictor of long-term outcome in patients with non-alcoholic fatty liver disease. *Aliment Pharmacol Ther*. 2019;49(9):1214–22.
- Buzzetti E, Tsochatzis EA. Letter: use of collagen proportionate area to quantify liver fibrosis and predict clinical outcomes non-alcoholic fatty liver disease-authors' reply. *Aliment Pharmacol Ther*. 2019;50(3):339.
- Calvaruso V, Burroughs AK, Standish R, Manousou P, Grillo F, Leandro G, et al. Computer-assisted image analysis of liver collagen: Relationship to ISHAK scoring and hepatic venous pressure gradient. *Hepatology*. 2009;49(4):1236–44.
- Tsochatzis E, Bruno S, Isgro G, Hall A, Theocharidou E, Manousou P, et al. Collagen proportionate area is superior to other histological methods for sub-classifying cirrhosis and determining prognosis. *J Hepatol*. 2014;60(5):948–54.
- Israelsen M, Guerrero Misas M, Koutsoumourakis A, Huang Y, Thiele M, Hall A, et al. Collagen proportionate area predicts clinical outcomes in patients with alcohol-related liver disease. *Aliment Pharmacol Ther*. 2020;52(11–12):1728–39.
- Papatheodoridi M, Hall AR, Rodríguez-Perálvarez M, Pieri G, Germani G, Gale JD, et al. Histological sub-classification of cirrhosis using collagen proportionate area in patients with chronic hepatitis C. *Liver Int*. 2021;41(7):1608–13.
- Isgro G, Luong T, Andreaana L, Garcovich M, Maimone S, Manousou P, et al. PP-011 Collagen proportionate area: a continuous quantitative of histological collagen has the best correlation with transient elastography. *Gut*. 2010;59(Suppl 1):A44.
- Restellini S, Goossens N, Clément S, Lanthier N, Negro F, Rubbia-Brandt L, et al. Collagen proportionate area correlates to hepatic venous pressure gradient in non-abstinent cirrhotic patients with alcoholic liver disease. *World J Hepatol*. 2018;10(1):73–81.
- Standish RA, Cholongitas E, Dhillon A, Burroughs AK, Dhillon AP. An appraisal of the histopathological assessment of liver fibrosis. *Gut*. 2006;55(4):569–78.
- Pinzani M, Luong TV. Pathogenesis of biliary fibrosis. *Biochim Biophys Acta Mol Basis Dis*. 2018;1864(4):1279–83.
- Theise ND. Histopathology of alcoholic liver disease. *Clin Liver Dis*. 2013;2(2):64–7.
- Lo RC, Kim H. Histopathological evaluation of liver fibrosis and cirrhosis regression. *Clin Mol Hepatol*. 2017;23(4):302–7.
- Pinzani M, Rombouts K. Liver fibrosis: from the bench to clinical targets. *Dig Liver Dis*. 2004;36(4):231–42.
- de Franchis R. Expanding consensus in portal hypertension. *J Hepatol*. 2015;63(3):743–52.
- Schwabl P, Laleman W. Novel treatment options for portal hypertension. *Gastroenterol Rep*. 2017;5(2):90–103.
- Nakamoto K, Takayama F, Mankura M, Hidaka Y, Egashira T, Ogino T, et al. Beneficial effects of fermented green tea extract in a rat model of non-alcoholic steatohepatitis. *J Clin Biochem Nutr*. 2009;44(3):239–46.
- Takayama F, Egashira T, Kawasaki H, Mankura M, Nakamoto K, Okada S, et al. A novel animal model of nonalcoholic steatohepatitis (NASH): Hypoxemia enhances the development of NASH. *J Clin Biochem Nutr*. 2009;45(3):335–40.
- Königshofer P, Brusilovskaya K, Schwabl P, Podesser BK, Trauner M, Reiberger T, et al. Invasive hemodynamic characterization of the portal-hypertensive syndrome in cirrhotic rats. *JoVE*. 2018:57261.
- Reiberger T, Ferlitsch A, Payer BA, Pinter M, Schwabl P, Stift J, et al. Noninvasive screening for liver fibrosis and portal

- hypertension by transient elastography—A large single center experience. *Wien Klin Wochenschr.* 2012;124(11–12):395–402.
27. Reiberger T, Schwabl P, Trauner M, Peck-Radosavljevic M, Mandorfer M. Measurement of the hepatic venous pressure gradient and transjugular liver biopsy. *J Vis Exp.* 2020:e58819.
 28. Schwabl P, Bota S, Salz P, Mandorfer M, Payer BA, Ferlitsch A, et al. New reliability criteria for transient elastography increase the number of accurate measurements for screening of cirrhosis and portal hypertension. *Liver Int.* 2015;35(2):381–90.
 29. Blendis L, Wong F. The hyperdynamic circulation in cirrhosis: an overview. *Pharmacol Ther.* 2001;89(3):221–31.
 30. Garcia-Tsao G. Portal hypertension. *Curr Opin Gastroenterol.* 2006;22(3):254–62.
 31. Reiberger T, Püspök A, Schoder M, Baumann-Durchschein F, Bucsecs T, Datz C, et al. Austrian consensus guidelines on the management and treatment of portal hypertension (Billroth III). *Wien Klin Wochenschr.* 2017;129(Suppl 3):135–58.
 32. Reiberger T, Ulbrich G, Ferlitsch A, Payer BA, Schwabl P, Pinter M, et al. Carvedilol for primary prophylaxis of variceal bleeding in cirrhotic patients with haemodynamic non-response to propranolol. *Gut.* 2013;62(11):1634–41.
 33. Kendall RL, Wang G, Thomas KA. Identification of a natural soluble form of the vascular endothelial growth factor receptor, FLT-1, and its heterodimerization with KDR. *Biochem Biophys Res Commun.* 1996;226(2):324–8.
 34. Roeckl W, Hecht D, Sztajer H, Waltenberger J, Yayon A, Weich HA, et al. Differential binding characteristics and cellular inhibition by soluble VEGF receptors 1 and 2. *Exp Cell Res.* 1998;241(1):161–70.
 35. Ferro D, Quintarelli C, Lattuada A, Leo R, Alessandrini M, Mannucci PM, et al. High plasma levels of von Willebrand factor as a marker of endothelial perturbation in cirrhosis: relationship to endotoxemia. *Hepatology.* 1996;23(6):1377–83.
 36. La Mura V, Reverter JC, Flores-Arroyo A, Raffa S, Reverter E, Seijo S, et al. Von Willebrand factor levels predict clinical outcome in patients with cirrhosis and portal hypertension. *Gut.* 2011;60(8):1133–8.
 37. Mandorfer M, Schwabl P, Paternostro R, Pomej K, Bauer D, Thaler J, et al. Von Willebrand factor indicates bacterial translocation, inflammation, and procoagulant imbalance and predicts complications independently of portal hypertension severity. *Aliment Pharmacol Ther.* 2018;47(7):980–8.
 38. Pak JM, Lee SS. Vasoactive effects of bile salts in cirrhotic rats: in vivo and in vitro studies. *Hepatology.* 1993;18(5):1175–81.
 39. Polio J, Groszmann RJ, Reuben A, Sterzel RB, Better OS. Portal hypertension ameliorates arterial hypertension in spontaneously hypertensive rats. *J Hepatol.* 1989;8(3):294–301.
 40. Costa D, Simbrunner B, Jachs M, Hartl L, Bauer D, Paternostro R, et al. Systemic inflammation increases across distinct stages of advanced chronic liver disease and correlates with decompensation and mortality. *J Hepatol.* 2021;74(4):819–28.
 41. Mehta G, Mookerjee RP, Sharma V, Jalan R. Systemic inflammation is associated with increased intrahepatic resistance and mortality in alcohol-related acute-on-chronic liver failure. *Liver Int.* 2015;35(3):724–34.
 42. Ferrusquía-Acosta J, Bassegoda O, Turco L, Reverter E, Pellone M, Bianchini M, et al. Agreement between wedged hepatic venous pressure and portal pressure in non-alcoholic steatohepatitis-related cirrhosis. *J Hepatol.* 2021;74(4):811–8.
 43. Navasa M, Parés A, Bruguera M, Caballería J, Bosch J, Rodés J, et al. Portal hypertension in primary biliary cirrhosis. Relationship with histological features. *J Hepatol.* 1987;5(3):292–8.
 44. Russell WMS, Burch RL. *The Principles of Humane Experimental Technique.* London: Methuen; 1959.
 45. Erratum to “FELASA recommendations for the health monitoring of mouse, rat, hamster, guinea pig and rabbit colonies in breeding and experimental units”. *Lab Anim.* 2014;49(1):88.

SUPPORTING INFORMATION

Additional supporting information may be found in the online version of the article at the publisher's website. Supplementary Material

How to cite this article: Königshofer P, Hofer BS, Brusilovskaya K, Simbrunner B, Petrenko O, Wöran K, et al. Distinct structural and dynamic components of portal hypertension in different animal models and human liver disease etiologies. *Hepatology.* 2022;75:610–622. <https://doi.org/10.1002/hep.32220>